Paper to be presented at "Antenna Measurement Techniques Association 30th Annual Symposium" (AMTA 2008), Boston, MA, USA, 16-21 November 2008, Paper No. A08-0107.

COMPACT RANGE EVALUATION BY GTD MODELLING[1]

Frank Jensen and Per Heighwood Nielsen

TICRA, Laederstraede 34, DK-1201 Copenhagen, Denmark
www.ticra.com

ABSTRACT

A compact antenna test range has been analysed for stray signals. The analysis is based on GTD ray tracing, i.e. obeying the reflection law in the chamber walls and assuming straight edges of reflectors and walls. Comparisons to an RCS as well as a time-domain measurement of the quiet-zone performance show good agreements with respect to identification of the ray paths of the stray signals. Rough estimates of the power loss at reflections and diffractions show acceptable agreements with the measured levels.

Keywords: Compact range modelling, GTD, Ray tracing.

1. Introduction

The Compact Payload Test Range (CPTR) at the European Space Research and Technology Centre (ESTEC) has been evaluated around its low frequency boundary. Two different methods have been applied.

The first method is an RCS measurement: A plane metallic screen (a mirror) is rotated in the quiet zone and the scattering back to the range feed is recorded. In this way, stray fields reaching the quiet zone are recorded when the mirror is in such an orientation that it reflects the fields back through the range reflectors to the feed.

The second method is a time domain measurement in which a pulse is sent from the feed and the response from an antenna in the quiet zone is recorded. Different scatterings reach the antenna with different time delays giving the path lengths of the signals.

A numerical modelling of the two measurement methods is presented in the following and has been used to identify the most important sources of scattering in the chamber. The modelling is based on ray tracing according to the rules of Geometrical Theory of Diffraction (GTD) and is carried out by the GRASP Multi-GTD add-on [1].

2. The range (CPTR)

The CPTR was the first large compact range designed as a compensated range, i.e. with a very low cross polarisation. The reflectors edges are supplied with 0.9 m serrations and the solid areas of sub- and main reflectors are 7.2 m and 7.9 m (respective widths) by 5.5 m. The main reflector (M) is mounted at the end of the chamber, cf. Figure 1, and the subreflector (S) is mounted to the one side in a niche with the feed (F) positioned opposite.

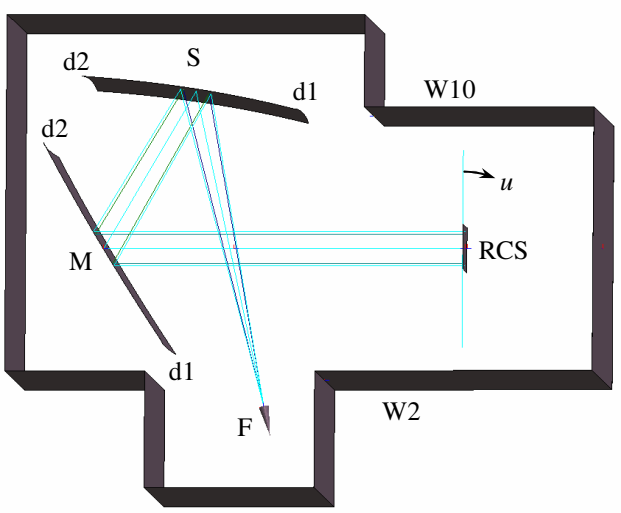

Figure 1 – Outline of the CPTR range with feed (F), sub- (S) and main (M) reflectors and the reflecting mirror (RCS) in the quiet zone.

The available measurements were carried out in order to investigate the range performance at frequencies near and below the lower limit for which the range was designed. A reduced performance of serrations and absorbers may therefore be expected.

3. GTD modelling of the range

The range is modelled by GTD and the reflectors are here taken to be solid also over the area with the edge serrations. Ordinary edge diffractions are thus assumed along the 'edges' formed by the tips of the serrations.

The modelling is here limited to rays in the horizontal centre plane of the range. Thus, reflections and diffractions in the vertical walls and vertical inward corners of the chamber are included.

[1] The work presented here has been carried out for the European Space Agency (ESA) on ESTEC Contract 18802-CCN2

4. The RCS measurements

In the RCS measurements, a mirror is mounted centrally in the quiet zone. The mirror is a plane, circular metallic screen of diameter 2 m (RCS, Figure 1). During the measurements this mirror is rotated the angle u around a vertical axis. In Figure 1, the mirror is shown at $u = 0°$.

The mirror will collect fields arriving to the quiet zone from specific direction given by twice the angle of rotation, and will reflect these fields back through the range reflectors to the feed where they are recorded. The mirror thus probes the quiet zone for horizontal stray signals.

In the model the direction of propagation is reversed. Rays are emitted from the feed within a narrow fan corresponding to the width of the mirror. The rays are traced through reflections in the sub- and main reflectors to the mirror in which they are reflected. When the mirror is rotated, the reflected fan of rays sweeps the chamber.

When this reflected fan hits a wall or a reflector it will be reflected again, and when it hits an edge - of a reflector or of the chamber - a diffraction is generated and these diffracted rays are traced to the feed position. This further ray-tracing may include several reflections but only one additional diffraction is included here. The reflections in the walls of the chamber are assumed specular, occurring at the base of the absorbers.

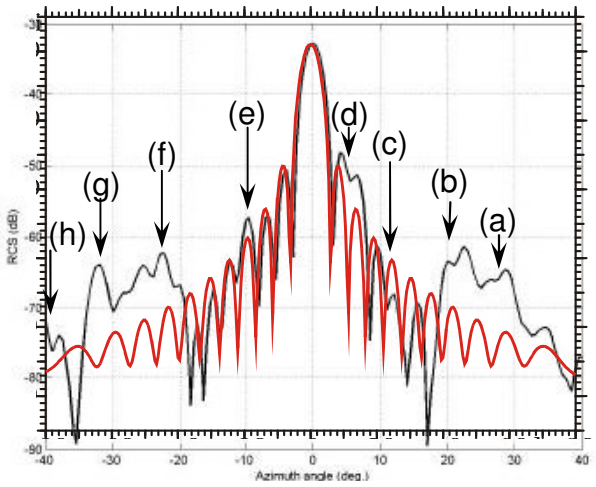

Figure 2 – RCS backscattering, measured (black) and ideal (red). The letters refer to the different versions of Figure 3.

The backscattering to the feed, measured at 1.7 GHz, is shown as function of the rotation angle, u, of the mirror in Figure 2 (black curve). For comparison, the red curve shows the ideal response, namely the pattern of a uniformly illuminated aperture with same diameter as the mirror. For this curve, the side lobes represent diffractions in the edges of the mirror, diffractions which are reflected back through the range reflectors to the feed.

In order to evaluate the undesired paths, the mirror is rotated in the model. The following Figures 3(a)-(h) shows the paths for those angles of rotation which generate rays reaching the feed within the time gating applied in the measurements (corresponds to –2 m/+7 m). All rays are drawn with a length of the nominal ray path, 76 m. This is the path length for $u = 0°$ from the feed over the reflectors to the mirror and back again.

The mirror rotates anti-clockwise in the figures corresponding to decreasing u. Rays which are solely reflected in the range are shown in cyan. Rays which are diffracted and then traced to the feed, are shown in various colours.

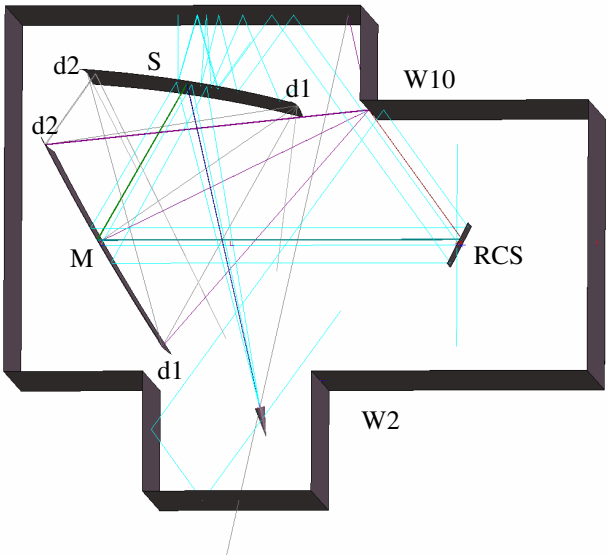

Figure 3(a) – Ray paths at $u = 28°$.

For rotation angles within $25° < u < 31°$, Figure 3(a), the corner of wall W10 is hit and diffractions from the corner reflects and diffracts in the chamber. Seven different ray paths are identified here but only one ray reaches the feed within the time gate. After the diffraction in wall W10 the ray diffracts in edge d2 of the main reflector and then reflects in the subreflector. As seen in the figure the drawn ray lacks a little (2.6 m) in reaching the feed, but the feed is reached within the time gate. The divergence factor shows that the ray is focused on the feed (the ray is caustic) which increases the level of the field.

Rays of the type shown in Figure 3(a) then contribute to the lobes marked by (a) in Figure 2. A similar correspondence exists between the different figures labelled Figure 3 and the lobe indications in Figure 2.

The ray path may in short be denoted W10d´ → Md2 → Sr + C where d denotes diffraction, the prime (´) denotes

that the diffraction is not near a reflection boundary, r denotes reflection and C denotes that the ray is caustic. The ray notations shall be applied in Section 5.

When the mirror is at angles in the range 18º < *u* < 23º, Figure 3(b), the reflections from the mirror hit edge d1 of the subreflector and causes a ray which diffracts in edge d2 of the main reflector. The ray then reflects in the subreflector to the feed. The level is high as the diffractions are close to specular reflections. The ray is designated Sd1 → Md2 → Sr.

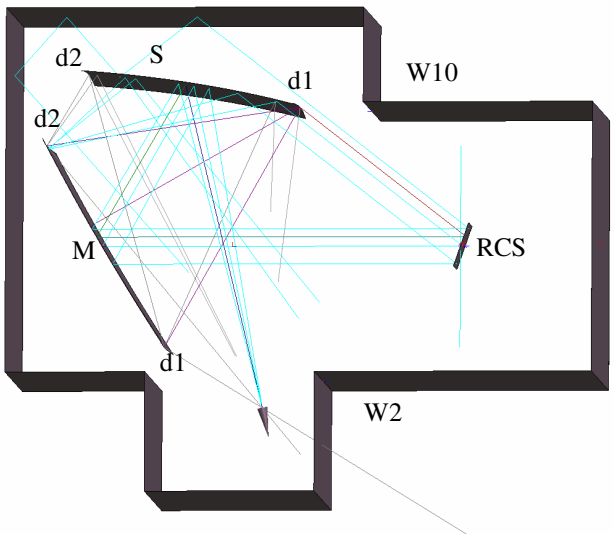

Figure 3(b) – Ray paths at *u* = 20º.

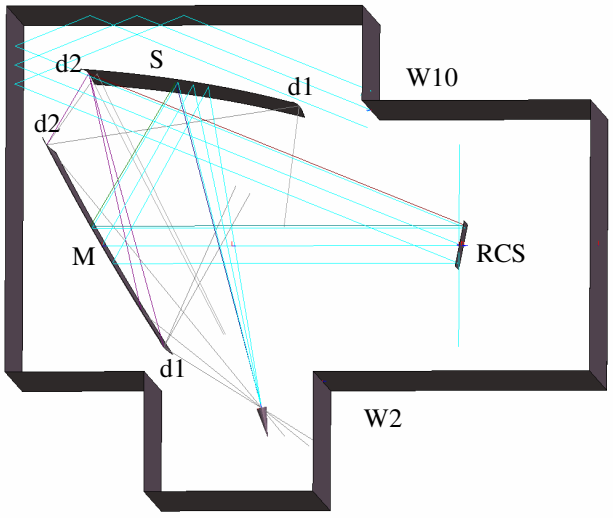

Figure 3(c) – Ray paths at *u* = 12º.

The next contributions arise when the reflections from the mirror illuminate edge d2 of the subreflector which happens for 11º < *u* < 13º, Figure 3(c), The most important ray is here diffracted in edge d2 of the subreflector, diffracted in edge d2 of the main reflector and then reflected in the subreflector. The ray is caustic and has importance though it is diffracted twice. The ray is designated Sd2´ → Md2´ → Sr + C.

For 6º < *u* < 7º, a triply reflected ray occurs. The ray from the mirror reflects in the main, the sub- and once again in the main reflector and was an unforeseen consequence of the wide scanning property of the range. The ray path is only 1.5 m longer than the nominal ray and the ray is caustic, Figure 3(d). The ray is designated Mr → Sr → Mr + C.

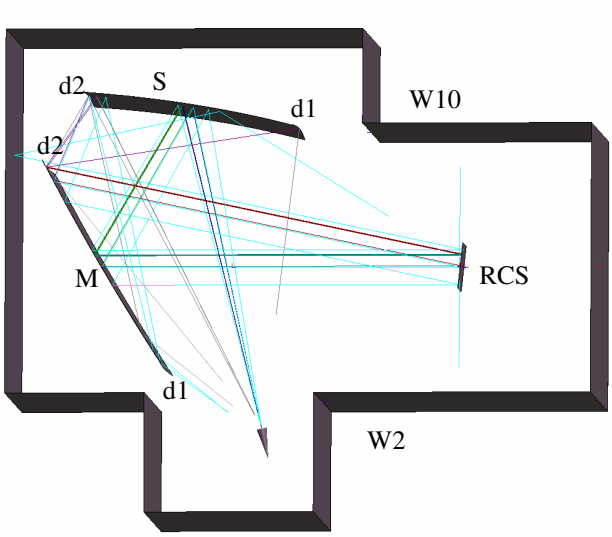

Figure 3(d) – Ray paths at *u* = 6º.

At *u* = 0º, the mirror reflects directly back into the feed along the nominal ray path, cf. Figure 1, causing the main lobe of the pattern in Figure 2. This ray is designated Mr → Sr + C.

A further rotation to *u* within the range –11º < *u* < –8º contributes with a diffraction in main reflector edge d1 followed by a reflection in the subreflector surface, Figure 3(e). The ray is caustic and causes a relatively strong response. The designation is Md1´ → Sr + C.

The next type of contributions are found in the range –23º < *u* < –20º. Several ray paths are possible through a diffraction in the CPTR corner of wall W2, Figure 3(f). The strongest contribution is, probably, when the diffraction is followed by diffraction in the main reflector edge d1 and reflection in the subreflector, a contribution which, again, is caustic. The ray is designated W2d´ → Md1´ → Sr + C.

In the range –35º < *u* < –33º only three rays are found of which the ray which reflects in wall W2, diffracts in

subreflector edge d1 and diffracts again in main reflector edge d1 has the strongest contribution, Figure 3(g), ray W2r → Sd1 → Md1´.

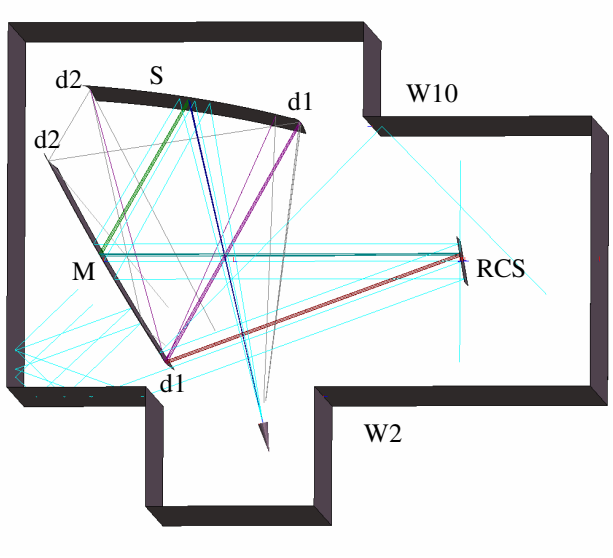

Figure 3(e) – Ray paths at *u* = –10º.

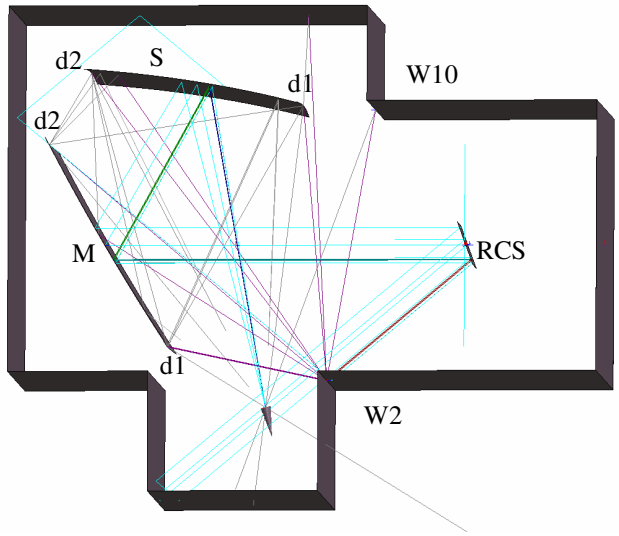

Figure 3(f) – Ray paths at *u* = –20º.

Finally, for *u* = –39º, we find a ray path with only wall reflections, in walls W2 and W8, Figure 3(h), ray W2r → W8r.

A good agreement is thus found between the geometrical ray paths in the RCS scattering and the angles of the mirror rotation for which stray signals occur. In spite of the uncertainty in positions of the diffracting serrated reflector edges the agreement is remarkable.

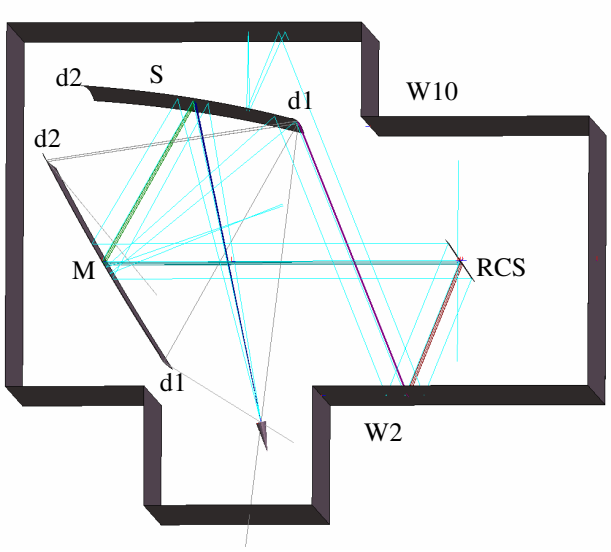

Figure 3(g) – Ray paths at *u* = –34º.

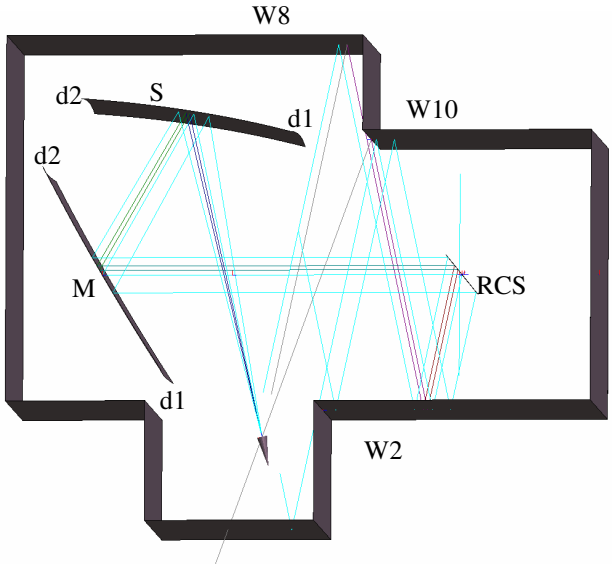

Figure 3(h) – Ray paths at *u* = –39º.

5. Field estimates

The field cannot be determined directly by GTD as absorber walls and the edges are not perfect conducting edges. However, some rough estimates may be carried out.

It has previously been demonstrated [2] that the scattering in range serrations may be equated with diffractions in straight edges but attenuated by 20 dB. In the present case the serrations are not optimal and the diffractions near a reflection boundary (d) is set to -10 dB (-18 dB when not near a boundary (d´)). Near the reflection boundary the

reflected field has same magnitude as the diffracted field, i.e. the reflection coefficient (r) may also be −10 dB in these regions, otherwise it should be set to zero.

In order to get some agreement with the measurements, a reflection in a wall of absorbers (W..r) is set to −5 dB and a diffraction in an absorber covered edge to −10 dB when it is not near a shadow or reflection boundary (W..d´). The caustic, C, is set to +10 dB. The amplitude of the feed pattern is assumed constant over the angles of interest.

That these values are reasonable can be seen from the levels of the different cases as given in the following Table I. For each case are, in the centre column, the ray path and its level estimated according to the above rules. The measured stray levels (difference between the curves in Figure 2) are stated in the right column.

Case /*u*	Ray path /estimated level (dB)	Measured, max/min (dB)
(a) 28º	W10d´→ Md2→ Sr + C −10 −10 −10 +10 = −20	–21/–25
(b) 20º	Sd1 → Md2 → Sr –10 –10 –10 = –30	–18/–28
(c) 12º	Sd2´ → Md2´→ Sr + C –18 –18 –10 +10 = –36	–26/–37
(d) 6º	Mr → Sr → Mr + C –10 –10 +0 +10 = –10	–7/–9
nominal 0º	Mr → Sr + C 0 +0 +10 = +10	+10
(e) –10º	Md1´ → Sr + C –18 –10 +10 = –18	–10/–26
(f) –20º	W2d´→ Md1´→ Sr + C –10 –18 –10 +10 = –28	–18/–25
(g) –34º	W2r → Sd1 → Md1´ –5 –10 –18 = –33	–20/–24
(h) –39º	W2r → W8r –5 –5 = –10	–27/–37

Table I – Estimated and measured levels of stray fields. Note that nominal (peak) is +10 dB.

A fine agreement is observed for the cases (a) – (f). For case (g) the predicted level is too low and in case (h) it is too high, however, the measured pattern increases for lower, not measured, angles.

6. The time domain measurements

The other measurement of the range performance was carried out in the time domain at 1.2 GHz. A shaped beam antenna with directivity about 15 dB and HPBW 15º (the AUT) was illuminated in the range with a pulse from the feed. The measured time response is shown in Figure 4 (the resolution is 0.75 m).

The nominal signal is received at a time which transformed to a path length corresponds to a distance from the feed of 38 m, (D) in Figure 4. Other signals are received earlier (shorter paths) as well as later (longer paths).

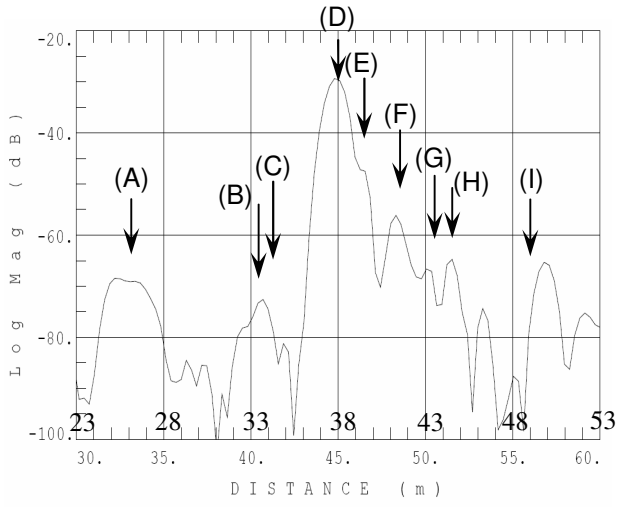

Figure 4 – Time response at AUT.

A ray-tracing analysis for rays emitted from the feed and scattered in the range has been carried out as shown in Figure 5. Reflections in the reflectors and the walls, and at most two diffractions in either the edges of the reflectors or in the inner corners of the chamber are included and the ray tracing shows that several rays propagate from the feed to the centre of the quiet zone. All rays in the figure are drawn with a total length of 38 m (the length of the nominal ray).

The ray paths cannot be analyzed from the figure alone. Sorting the rays by length and expected importance (reflections rather than diffractions) results in the following list of ray paths. The letters, (A) etc., correspond to the designations of the pulses in Figure 4. After each ray description, the measured field level according to Figure 4 is given and, in parenthesis, the estimated field level following the same rules as in Table I:

(A) Not identified in the model. Could be due to a diffraction in edge d1 of the subreflector followed by a scattering in the back structure of the subreflector, –40 dB.

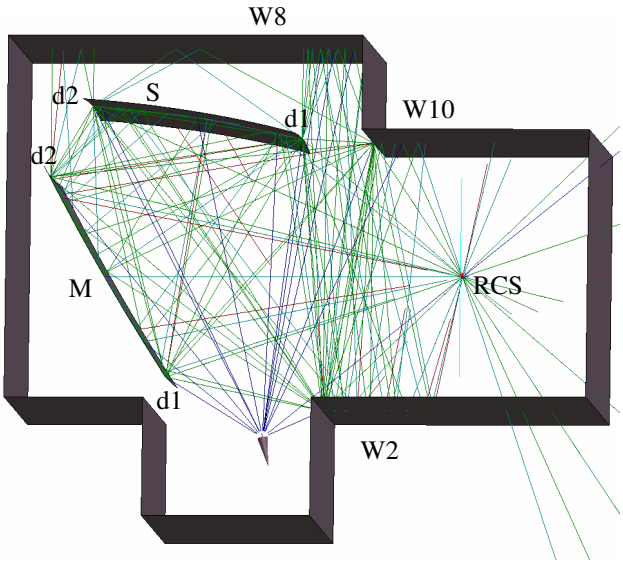

Figure 5 – Ray paths from the feed to the quiet zone.

(B) Diffraction in main reflector edge d2, –47 dB (Md2´; –18 dB).

(C) Diffraction in subreflector edge d2, –42 dB (Sd2´; –18 dB).

(D) Reflections in sub- and main reflector (the nominal ray), 0 dB (Sr → Mr; 0 dB).

(E) Reflections/diffractions in main, sub- and main reflector (paths close to that of the triply reflected ray), –18 dB (Md2 → Sr → Mr; –30 dB).

(F) Diffraction in edge d1 of the subreflector followed by reflection in wall W2, –25 dB (Sd1´ → W2r; –23 dB).

(G) Diffraction in edge d1 of the subreflector, next reflection in the central part of the main reflector and, finally, diffraction either in the same edge of the subreflector or in the corner of wall W2, –38 dB (Sd1 → Mr → Sd1; –36 dB).

(H) Diffraction, either in edge d1 of the subreflector or in the corner of wall W10, followed by reflection in wall W2 and reflection in wall W10, –35 dB (Sd1 → W2r → W10r; –28 dB)

(I) Reflection in wall W8 followed by diffraction in the corner of wall W10 and reflection in the main reflector, –35 dB (W8r → W10d´ → Mr; –25 dB).

Contributions with other path lengths have not been found.

The pulse positions are predicted well but the measured pulse levels only agree for a few cases, (F) and (G). For the other cases the estimates are either too high (by about 10 dB, (H) and (I), or 25 dB, (B) and (C)) or too low (by 12 dB, (E)).

For simplicity, only rays in the horizontal plane have been included in the model. This is a coarse simplification as the horizontal plane has no preferences in the time-domain measurement as was the case for the RCS measurements.

7. Conclusions

A compact antenna test range has been evaluated by means of ray propagation based on GTD. It has been demonstrated that the stray fields recorded in an RCS measurement of the back scattering from a mirror rotated in the quiet zone may be explained in this way. Also the pulses reaching the quiet zone as found in a time-domain measurement shows a good agreement with the GTD ray model. It is observed that the two methods supplement each other in the way the stray signals are identified.

It is found that the inward corners of the chamber contribute for several ray paths such as diffraction in a corner followed by reflections in one of the range reflectors. This illustrates that when a structure is erected in a range in order to reduce a direct radiation into the quiet zone from the feed (or an undesirable scattering from a range reflector) then rays are scattered into other directions causing other disturbances in the quiet zone.

Due to the low frequencies the absorbers apparently attenuate the signal by less than 5 dB at reflections. The diffractions in the serrated edges of the reflectors also have a considerable contribution with a diffraction level only 10 dB down. This is partly due to the applied low frequencies for which the serrations of the reflectors in fact are too short in terms of wavelengths.

The modelling of the range is simple as the serrations of the reflectors as well as the thickness of the absorbers are neglected. Nevertheless, the determined ray paths are in good agreement with the measurements, and the estimated field levels based on simple reflection and diffraction coefficients are reasonable for most of the ray paths, especially in the RCS measurement for which the modelling of only horizontal rays is most realistic.

References

[1] "GRASP9 Multi GTD", Technical Description, TICRA, Copenhagen, Denmark, May 2008.

[2] Jensen, F., Giauffret, L. and Marti-Canales, J, "Modelling of compact range quiet-zone fields by PO and GTD", 21rd *Proceedings of the Antenna Measurements Techniques Association* (AMTA-1999), Monterey Bay, CA, pp. 242-247, October 1999.